Relativistically Parameterized Extended Hückel Calculations. 13. Energy Bands for Uranium Compounds UB_2, UB_4, UC, UBC, and UPt_3

LAWRENCE L. LOHR

Department of Chemistry, University of Michigan, Ann Arbor, Michigan 48109

Abstract

The extension of the relativistically parameterized extended Hückel method REX to systems with translational symmetry is reviewed. This extension (REXBAND) is then applied to the description of the electronic structures of a number of heavy-element solids, namely UB_2, UB_4, UC, UBC, and UPt_3.

Introduction

In 1979 we outlined [1] a relativistically parameterized version of the extended Hückel molecular orbital method which we entitled REX. The method differs from standard extended Hückel schemes [2,3] in that it employs an atomic $|lsjm\rangle$ complex spin-orbital basis rather than a real basis without spin. This complex basis, when combined with the standard Hückel assumption of effective Hamiltonian matrix elements being proportional to the corresponding overlap matrix elements, permits the systematic incorporation of spin-orbit coupling into the calculations. In addition the energy parameterization and choice of orbital exponents may be taken to reflect the other two important relativistic effects [4–7] in atomic structure, namely the contraction and stabilization of those orbitals of low total angular momentum, particularly $s_{1/2}$ and $p_{1/2}$ levels, and the self-consistent expansion and destabilization of those orbitals of high total angular momentum. The REX method [1,7,8] has been used in a number of studies [9–19] of the electronic structure of compounds containing one or more elements of high atomic number; these include studies of actinide and lanthanide complexes, [10,15,17,19] main-group anionic clusters, [12] and nuclear spin-spin couplings [11,13,14].

In Part 11 of this series we outlined [18] the adaptation of the REX method to the description of systems with translational symmetry in one, two, or three dimensions, this adaptation thus permitting application of the REX method to polymers and solids with periodic boundary conditions. The resulting method was called REXBAND and is simply a relativistically parameterized variant of the tight-binding extended Hückel method for periodic systems which has proven so useful [20–22] in describing the electronic and geometric structures of a very large variety of materials. In Part 11 we also presented REXBAND energy bands and densities of states (DOS) for the helical structure of elemental tellurium and the simple cubic structure

International Journal of Quantum Chemistry: Quantum Chemistry Symposium 25, 121–130 (1991)

CCC 0020-7608/91/010121-10$04.00

of elemental polonium. Comparison of the results obtained with relativistic and with nonrelativistic parameters led to an interpretation of the polonium structure as a spin-orbit stabilized high-symmetry structure (coordination number of 6) and the tellurium structure as a reduced symmetry (coordination number of 2 with 4 next-nearest neighbors) variant. The structural differences were thus interpreted as reflecting the relative strengths of the spin-orbit splittings of the np shells (n = 5, 6 for Te, Po) and of the localization of the np orbitals by covalent bond formation.

In the present study we explore the application of the REXBAND method to a number of heavy-elemental solids, namely the refractory compounds UB_2, UB_4, UC, and UBC, as well as the heavy-fermion compound UPt_3.

Method

The REXBAND method may be easily described, as it is simply an extension of the REX method with its $|lsjm\rangle$ complex spin-orbital basis to periodic systems via the introduction of Bloch functions $\phi_\alpha(\mathbf{r},\mathbf{k})$, where

$$\phi_\alpha(\mathbf{r},\mathbf{k}) = \sum e^{i\mathbf{k}\cdot\mathbf{R}_{\alpha j}} f_\alpha(\mathbf{r} - \mathbf{R}_{\alpha j}) , \tag{1}$$

in which $\mathbf{k}$ is the wave vector, $\mathbf{R}_{\alpha j}$ is the position in cell j of the atom with orbital f_α of type α, and the summation is over cells.

The actual molecular orbitals (MOs) for the periodic system are given by solution of the generalized secular equation

$$\mathbf{H}(\mathbf{k})\mathbf{C}(\mathbf{k}) = \mathbf{S}(\mathbf{k})\mathbf{C}(\mathbf{k})\lambda^D(\mathbf{k}) , \tag{2}$$

where $\mathbf{C}(\mathbf{k})$ is the matrix whose columns are the complex eigenvectors, $\lambda^D(\mathbf{k})$ is the real diagonal matrix of eigenvalues, $\mathbf{S}(\mathbf{k})$ is the $n \times n$ overlap matrix given by

$$\mathbf{S}(\mathbf{k}) = \sum e^{i\mathbf{k}\cdot\mathbf{R}_j}\mathbf{S}^j , \tag{3}$$

in which $\mathbf{S}^j$ is the $n \times n$ overlap matrix between the n functions in the reference cell ($j = 0$) and the translationally related n functions in the jth cell, $\mathbf{R}_j$ is the vector location of the jth cell, and $\mathbf{H}(\mathbf{k})$ is the effective one-electron Hamiltonian matrix similarly constructed as

$$\mathbf{H}(\mathbf{k}) = \sum e^{i\mathbf{k}\cdot\mathbf{R}_j}\mathbf{H}^j . \tag{4}$$

The procedure is first to construct the set $\{\mathbf{S}^j\}$ of overlap matrices between real AOs in the reference cell ($j = 0$) and the jth cell, second to obtain $\mathbf{S}(\mathbf{k})$ in the real basis via (3), and finally to transform $\mathbf{S}(\mathbf{k})$ to the complex $|lsjm\rangle$ basis. The Hamiltonian matrix $\mathbf{H}(\mathbf{k})$ is then constructed directly in the $|lsjm\rangle$ basis by standard extended Hückel assumptions. It is useful, however to note here how $\mathbf{H}(\mathbf{k})$ is in effect constructed cell by cell: for $\mathbf{H}^0$ (interactions within the reference cell), the diagonal elements $H^0_{\alpha\alpha}$ are input parameters, and the off-diagonal elements $H^0_{\alpha\beta}$ are related to the corresponding overlap matrix elements via

$$H^0_{\alpha\beta} = (1.75/2)(H^0_{\alpha\alpha} + H^0_{\beta\beta})S^0_{\alpha\beta} , \qquad \alpha \neq \beta . \tag{5}$$

The diagonal and off-diagonal elements of $\mathbf{H}^j$ ($j \neq 0$) then become

$$H^{j}_{\alpha\alpha} = 1.75 H_{\alpha\alpha} S^{j}_{\alpha\alpha} , \tag{6a}$$

$$H^{j}_{\alpha\beta} = (1.75/2)(H^{0}_{\alpha\alpha} + H^{0}_{\beta\beta}) S^{j}_{\alpha\beta} , \qquad \alpha \neq \beta \tag{6b}$$

such that $H_{\alpha\alpha}(\mathbf{k})$ is related to $S_{\alpha\alpha}(\mathbf{k})$ via

$$H_{\alpha\alpha}(\mathbf{k}) = H^{0}_{\alpha\alpha}[1 + 1.75(S_{\alpha\alpha}(\mathbf{k}) - 1)] \tag{7}$$

and $H_{\alpha\beta}(\mathbf{k})$ is related to $S_{\alpha\beta}(\mathbf{k})$ via

$$H_{\alpha\beta}(\mathbf{k}) = (1.75/2)(H^{0}_{\alpha\alpha} + H^{0}_{\beta\beta}) S_{\alpha\beta}(\mathbf{k}) , \qquad \alpha \neq \beta . \tag{8}$$

As we have previously outlined [1], the overlap matrix in the $|lsjm\rangle$ basis is central to the REX method and is calculated by supplying as input data *two* sets of real atomic orbitals for each atom. The first and second sets consist of those orbitals whose radial functions are later associated with the $j = l - 1/2$ and $j = l + 1/2$ orbitals, respectively. The standard methods for calculating the real overlap matrix in the real atomic orbital (AO) basis are employed. A unitary transformation is then used to construct the overlap matrix in the desired basis. For example, the three real p AOs of the first set are used to construct the two functions $j = 1/2$, $m = \pm 1/2$, while the second set of three real p AOs are used to construct the four functions $j = 3/2$, $m = \pm 3/2, \pm 1/2$. This is carried out separately for each atom-pair block of the original real overlap matrix and separately for α and β spins. In the REXBAND procedure this transformation follows the construction of $\mathbf{S}(\mathbf{k})$ according to (3); that is, the complex $\mathbf{S}(\mathbf{k})$ is obtained via (3) from a set of real $\mathbf{S}^{j}$ for a suitably chosen range of cells neighboring the reference cell, and then the REX transformation to $\mathbf{S}(\mathbf{k})$ in the $|lsjm\rangle$ basis is made. The construction of $\mathbf{H}(\mathbf{k})$ in REXBAND is then made directly in the $|lsjm\rangle$ basis using (4)–(8). Minor computational details are skipped here, but it should be noted that population analysis routines must be modified to account for the diagonal elements of $\mathbf{S}(\mathbf{k})$ not always being unity.

The REX parameters listed in Table I for B, C, Pt, and U are primarily the default REX values, that is, orbital energies α taken as Desclaux's atomic Dirac–Fock orbital energies [23] and single-zeta Slater exponents ζ fitted to Desclaux's electron mean radii $\bar{r}$ values [23] by $\zeta = (n + 1/2)/\bar{r}$, where n is the principal quantum number. We also used the Pt parameter set (double-zeta for 5d) of Silvestre and Hoffmann, [24] and the U set of Pyykkö et al. [19].

Since the default α values (Table I) for $U(5f_{5/2})$ and $U(5f_{7/2})$, -9.44 and -8.70 eV respectively, are above the C(2p) value of -11.07 eV but below that for B(2p) of -8.43 eV, a simple filling of REXBAND MOs will result in very different U(5f) occupancies for carbides vs. borides. This is a general problem in applying a one-electron method to systems in which one or more atoms have a partially filled AO nearly degenerate with AOs of other atoms. Rather than graft intra-atomic electron repulsions onto the method, we simply fix the occupancy of such shells, thus obtaining a Fermi energy ϵ_F and charge distribution conditional upon the choice. For the U compounds we choose occupancies $5f^{n}_{5/2}\ 5f^{0}_{7/2}$ with $n = 4$, 3, or 2; these choices correspond to U^{2+}, U^{3+}, and U^{4+}, respectively, *if* there are no electrons

TABLE I. REXBAND parameters.[a]

Element	AO[b]	α (eV)	ζ
B	2s	−13.47	1.265
	2p*	−8.43	1.134
	2p	−8.43	1.134
C	2s	−19.39	1.577
	2p*	−11.07	1.435
	2p	−11.07	1.434
Pt	6s	−7.73 (−9.29)[c]	2.071 (2.554)[d]
	6p*	−4.49 (−4.84)	1.835 (2.554)
	6p	−3.95 (−4.30)	1.621 (2.554)
	5d*	−12.20 (−12.16)	3.415
	5d	−10.70 (−10.66)	3.245
U	7s	−5.51	1.728
	6p*	−36.55	3.907
	6p	−26.79	3.425
	6d*	−5.24	2.062
	6d	−4.99	1.974
	5f*	−9.44	3.866
	5f	−8.70	3.761

[a] Orbital energies α in eV and Slater exponents ζ.

[b] The * denotes AO with $j = l - 1/2$.

[c] Orbital energies from Ref. [24] adjusted by calculated spin-orbit splittings from Ref. [23].

[d] Slater exponents from Ref. [24]; the double-ζ 5d function has $\zeta_1 = 6.103$ ($c_1 = 0.6334$) and $\zeta_2 = 2.696$ ($c_2 = 0.5513$).

in the U(7s) and (6d) AOs. However, the U(7s) and (6d) occupancies are not fixed, so that our assumption about the U($5f_{5/2}$) occupancy does not fix the Mulliken charges. We also have the options of carrying out calculations for the separate sublattices (U or B/C) or for the compounds with designated AOs, such as U(5f), simply deleted. Finally for purposes of this study we take ϵ_F values as the energy of the highest occupied MO (subject to occupancy constraints) whether or not there is an energy gap at this level.

Results and Discussion

UB_2

The compound UB_2 crystallizes [25,26] in the trigonal space group D^3_{3d} ($P\bar{3}m1$) with $Z = 1$. Hexagonal layers of U atoms alternate with graphitelike hexagonal layers of B atoms; the B layers are eclipsed rather than staggered as are the C layers in graphite, so that each U atom has 12 B nearest neighbors as the vertices of a hexagonal prism. The U–B distance is $(a^2/3 + c^2/4)^{1/2} = 2.691$ Å, the B–B distance is $a/3^{1/2} = 1.807$ Å, and the U–U distance is $a = 3.130$ Å, a value comparable to the 3.01 Å separation in bcc γ–U, but definitely larger than the 2.76 and 2.85 Å separations in α–U (the U–U distance between planes in UB_2 is $c = 3.989$ Å).

Calculations at 40 randomly selected k-points produce the density-of-states histogram shown in Figure 1 together with that for the B sublattice. Assigned occupancies of 4, 3, and 2 for $U(5f_{5/2})$, corresponding to charges of U^{2+}, U^{3+}, and U^{4+} without contributions from U(7s) and (6d) occupancy, lead to ϵ_F values of −6.1, −5.1, and −3.8 eV, respectively; ϵ_F values for the B sublattice alone are −6.8 and −3.8 eV for B_2^{2-} and B_2^{3-}, respectively (the value for B_2^{4-} is above zero), indicating that the U(7s) and (6d) AOs stabilize the excess electron count (3 per U atom) corresponding to a $U^{3+}(5f_{5/2}^3)$ core, but not the count (2 per U atom) corresponding to $U^{2+}(5f_{5/2}^4)$. There is no appreciable gap in the UB_2 DOS at any of the above ϵ_F values or in the B sublattice DOS.

UB_4

The compound UB_4 crystallizes [27,28] in the tetragonal space-group D_{4h}^5 (P4/mbm) with $Z = 4$. Planes of U atoms alternate with layers of B_6 octahedra linked by B_2 units, with each end of a B_2 unit bonded to a vertex of two different B_6 units. The U–U distances are 3.640 Å in the plane perpendicular to c and 3.978 Å parallel to c.

As expected from earlier theoretical studies [29] of MB_6 and MB_{12} compounds, extra electrons are needed to stabilize the B sublattice. Bullett has concluded [30] from pseudopotential calculations on LaB_4, isostructural with UB_4, that a quasi-filled-shell with 60 valence electrons per unit cell, corresponding to B_{16}^{12-}, and 4 more than the 56 needed for $2(B_6^{2-} + B_2^{2-}) = B_{16}^{8-}$, is stabilized by interactions with metal d AOs. For the B sublattice alone, we obtain a DOS (Fig. 2) from 20 k points having a minimum for 56 electrons ($\epsilon_F = -6.3$ eV) and also a small gap (about

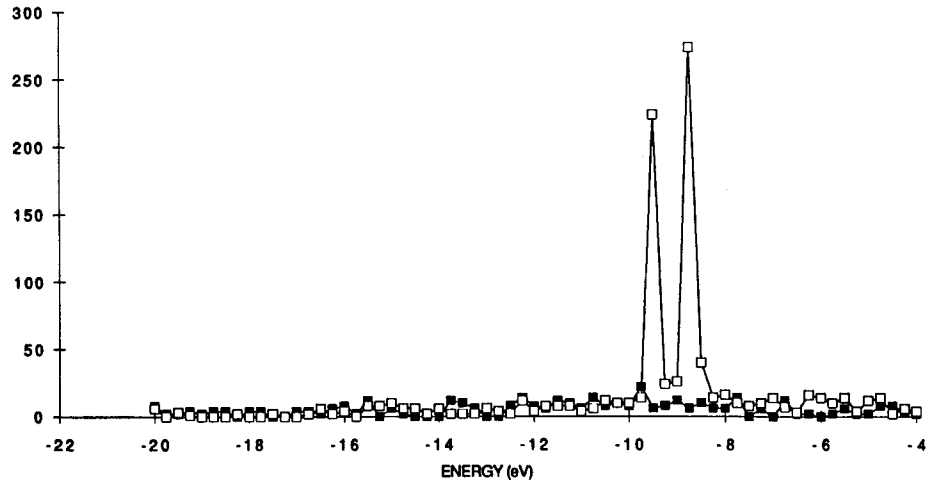

Figure 1. Density-of-states histogram (DOS) vs. energy in eV for UB_2. Solid squares denote DOS for B sublattice (no U AOs), open squares for the compound (with U AOs). The corelike U(6p) levels are not shown.

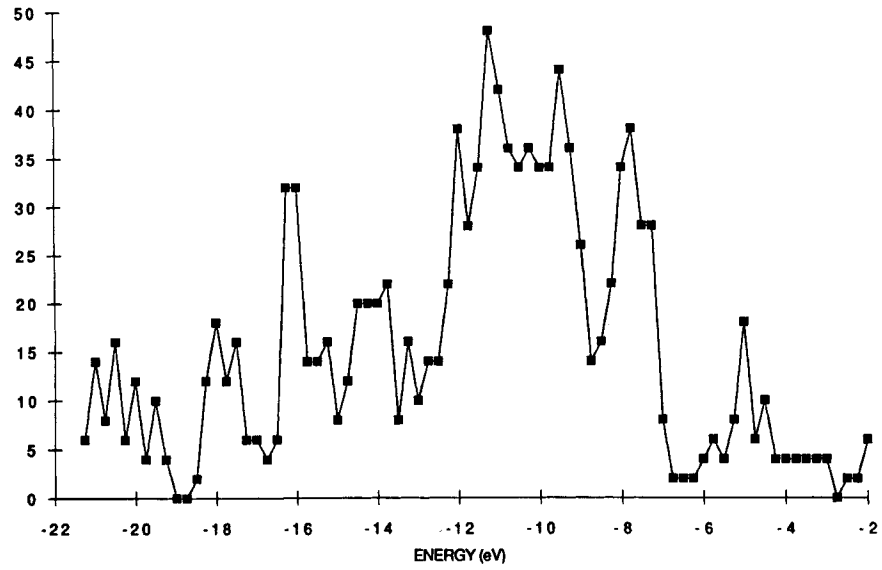

Figure 2. DOS curve as in Figure 1 but for the B sublattice (no U AOs) of UB_4.

0.5 eV) for 60 electrons ($\epsilon_F = -3.0$ eV). We find the charge distribution for the B sublattice to be relatively insensitive to the k value; for B_{16}^{12-} the charges are -0.43 for each apical B of the B_6 units, -0.46 for each equatorial B of the B_6 units, and -1.65 for each B of the B_2 units. By contrast, for the 56-electron B_{16}^{8-} unit these charges are -0.28, -0.34, and -1.04, respectively, indicating that much of the electron density for the 4 extra electrons in B_{16}^{12-} is associated with the π^* MO of the B_2 units, the MO being stabilized by interaction with the B_6 units. Thus both 56 and 60 appear to be "magic numbers" even without interactions with metal AOs, with 60 being the electron number corresponding to an M^{+3} boride.

Calculations including U AOs were made at 40 randomly selected k-points, with resulting ϵ_F values being -6.9, -6.0, and -3.8 eV, for assigned $U(5f_{5/2})$ occupancy of 4, 3, and 2, respectively. Again we note a major stabilization (3 eV) when there are 3 excess electrons per U to be distributed over U(7s), U(6d), and B AOs, as opposed to their being solely on the B sublattice. For UB_4, unlike UB_2, there is a slight stabilization for 2 excess electrons per U, but nonetheless a description in terms of a $U^{3+}(5f_{5/2}^3)$ core seems preferable. We also note that the UB_4 DOS (not shown) has no gap at the -6.0 eV ϵ_F value corresponding to U^{3+} cores.

UC

The compound UC has the cubic rock-salt structure, [26,31] that is, space group O_h^5 (Fm3m) with $Z = 4$. Each U atom is thus surrounded by 6 C atoms at a distance of $a/2 = 2.481$ Å, with the U–U and C–C distances each being $a/2^{1/2} = 3.509$ Å. The structure may be viewed as a "bloated" fcc U with C's in the octahedral holes.

Figure 3 shows the DOS obtained from 40 randomly selected k points. Again considering cores with fixed U($5f_{5/2}$) occupancies of 4, 3, and 2, we obtain ϵ_F values of −8.0, −7.2, and −6.1 eV, respectively. Since C(2p) lies below U($5f_{5/2}$), these values are not reflecting a true destabilization of the C sublattice for which ϵ_F ranges from −11.3 eV for C^0 to −9.8 eV for C^{4-}. Instead these C values reflect increasing occupancy of weakly interacting C(2p) AOs, which are an electron sink in our one-electron model. Interactions between U(7s) and (6d) with C(2p) are making ϵ_F higher than the C sublattice values but lower than the 7s and 6d α values of −5.5 to −5.0 eV (Table I).

UBC

The compound UBC crystallizes [26] in the orthorhombic space group D_{2h}^{17} (Cmcm) with $Z = 4$. There are BC pairs, with a separation of 1.65 Å. The U–U distance is large (3.58, 3.74 Å), while the U–B (2.57, 2.75 Å) and U–C (2.35, 2.40 Å) distances are comparable to those found in other structures. The DOS (not shown) obtained from 40 k points yields ϵ_F values at −7.9, −7.1, and −5.7 eV for assigned U($5f_{5/2}$) occupancy of 4, 3, and 2, respectively. These values are somewhat higher than the BC sublattice values of −9.6, −7.8, and −5.8 for the same number of excess electrons (BC^{2-}, BC^{3-}, and BC^{4-}, respectively). We note that the mean of the 2p α's for B and C is −9.75 eV (Table I), nearly degenerate with the −9.4 eV value for U($5f_{5/2}$). Thus the sublattice is not acting significantly as a source or a sink for electrons.

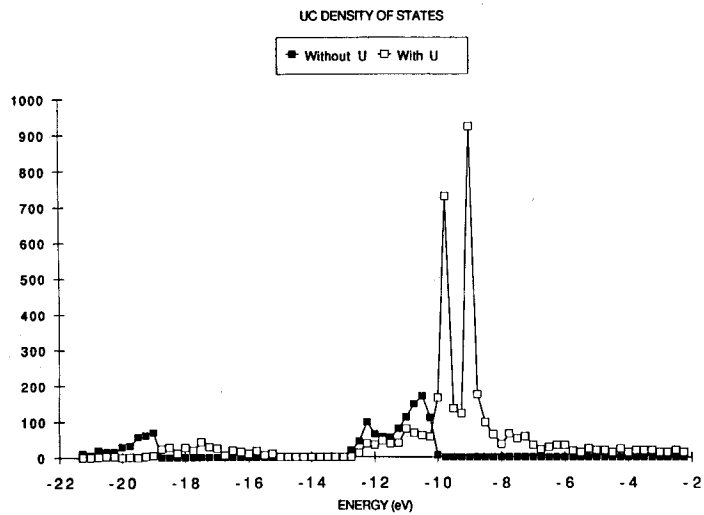

Figure 3. DOS curves as in Figure 1 but for UC. Solid squares denote DOS for C sublattice, open squares for the compound.

UPt_3

The heavy-fermion [32] intermetallic UPt_3 crystallizes [33] in the hexagonal space group D^4_{6h} ($P6_3/mmc$) with $Z = 2$. The structure (Na_3As-type) may be viewed as hcp with each U having 12 Pt nearest neighbors at distances of 2.876 (within a layer) and 2.955 Å (to adjacent layers), and with each Pt having 2 U and 4 Pt neighbors in the hexagonal layer and another 2 U and 4 Pt nearest neighbors in adjacent layers. Thus each U atom is totally isolated from other U's, while each Pt has U for 4 of its 12 nearest neighbors. Figure 4 shows the DOS both for the Pt sublattice, which is simply a hcp Pt with one-fourth of the sites vacant, and for the compound. We have also obtained $\epsilon(k)$ along symmetry directions (not shown) for a model without U(5f) AOs. We find a Pt($5d_{5/2}$) band of approximately 1 eV width lying below (with the default parameterization) the U($5f_{5/2}$) energy of −9.44 eV. Typical average charges are only 0.2 for U and −0.06 for Pt, with the U($5f_{5/2}$) level having nearly 5 electrons, and ϵ_F being −9.5 eV. If instead a U($5f^3_{5/2}$) core is assumed, the ϵ_F value is −6.8 eV, comparable to that for the other U compounds studied. Dispersion of the low-energy Pt($5d_{3/2}$) band is minimal, while the U($5f_{5/2}$) level is intersected by a strongly dispersed conduction band constructed from U(7s), U(6d), and Pt(6s,6p) AOs. Thus the overall description resembles that reported by Albers et al. [34] as based on their relativistic linear muffin-tin calculations, namely a narrow spin-orbit-split U(5f) band at the Fermi energy just above a filled Pt(5d) band.

Summary

The REXBAND method is applied to the description of a number of solid U compounds, with the resulting densities of states being used to discuss their probable electronic structures. A description of the compounds in terms of an assigned $U^{3+}(5f^3_{5/2})$ core appears particularly reasonable, leading to highest occupied levels,

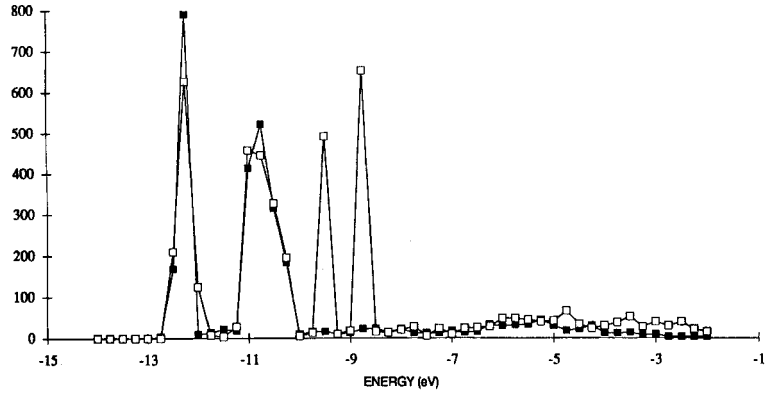

Figure 4. DOS curves as in Figure 1 but for UPt_3. Solid squares denote DOS for the Pt sublattice, open squares for the compound.

which we take to represent ϵ_F values, ranging from -5.1 eV for UB_2 to -7.2 eV for UC. The values are approximately 1 eV more negative if $U^{2+}(5f^4_{5/2})$ cores are assumed instead. By comparison, an isolated U^0 atom with a configuration $5f^3_{5/2}$ $7s^2_{1/2}$ $6d^1_{3/2}$ has, with our default parameterization, a $6d_{3/2}$ HOMO with $\alpha = -5.24$ eV. Another comparison is provided by bcc γ–U for which the U–U separation is 3.01 Å; the DOS obtained from 40 k points yields ϵ_F values of -4.8 and -3.8 eV for assumed $U(5f_{5/2})$ occupancies of 4 and 3, respectively. All of the compounds considered have larger U–U separations than γ–U, so that U–U interactions in them are less than in γ–U.

Acknowledgment

This paper is presented in the Sanibel 1991 Symposium on "Electron Deficient Compounds" in great appreciation to Professor William N. Lipscomb, Harvard University, for his stimulating guidance during the author's graduate student years 1959–63.

Bibliography

[1] L. L. Lohr and P. Pyykkö, Chem. Phys. Lett. **62**, 333 (1979) [REX part 1].
[2] R. Hoffmann, J. Chem. Phys. **39**, 1397 (1963).
[3] J. Howell, A. Rossi, D. Wallace, K. Haraki, and R. Hoffmann, QCPE **10** (Suppl.), 344 (1973).
[4] K. S. Pitzer, Acc. Chem. Res. **12**, 271 (1979).
[5] P. Pyykkö, and J.-P. Desclaux, Acc. Chem. Res. **12**, 276 (1979).
[6] P. Pyykkö, Chem. Rev. **88**, 563 (1988).
[7] P. Pyykkö, in *Methods in Computational Chemistry,* S. Wilson, Ed. (Plenum, New York and London, 1988) Vol. 2, pp. 136–226.
[8] L. L. Lohr, M. Hotokka, and P. Pyykkö, QCPE **12**, 387 (1980).
[9] L. L. Lohr, M. Hotokka, and P. Pyykkö, Int. J. Quantum Chem. **18**, 34 (1980) [REX part 2].
[10] P. Pyykkö and L. L. Lohr, Inorg. Chem. **20**, 1950 (1981) [REX part 3].
[11] P. Pyykkö and L. Wisenfeld, Mol. Phys. **43**, 557 (1981) [REX part 4].
[12] L. L. Lohr, Inorg. Chem. **20**, 4229 (1981) [REX part 5].
[13] P. Pyykkö, J. Organomet. Chem. **232**, 21 (1982) [REX part 6].
[14] A. Viste, M. Hotokka, L. Laaksonen, and P. Pyykkö, Chem. Phys. **72**, 225 (1982) [REX part 7].
[15] P. Pyykkö and L. Laaksonen, J. Phys. Chem. **88**, 4892 (1984) [REX part 8].
[16] S. Larsson and P. Pyykkö, Chem. Phys. **101**, 355 (1986) [REX part 9].
[17] L. L. Lohr and Y. Q. Jia, Inorg. Chim. Acta **119**, 99 (1986) [REX part 10].
[18] L. L. Lohr, Inorg. Chem. **26**, 2005 (1987) [REX part 11].
[19] P. Pyykkö, L. J. Laakkonen, and K. Tatsumi, Inorg. Chem. **28**, 1801 (1989) [REX part 12].
[20] J. K. Burdett, Prog. Solid State Chem. **15**, 17 (1984).
[21] T. A. Albright, J. K. Burdett, and M. H. Whangbo, *Orbital Interactions in Chemistry* (Wiley, New York, 1985).
[22] R. Hoffmann, *Solids and Surfaces: A Chemist's View of Bonding in Extended Structures* (VCH Publ., New York, 1988) and references contained therein.
[23] J.-P. Desclaux, At. Data Nucl. Data Tables **12**, 311 (1973).
[24] J. Silvestre, R. Hoffmann, Langmuir **1**, 621 (1985).
[25] L. Brewer, D. L. Sawyer, D. H. Templeton, and C. H. Dauben, J. Am. Chem. Soc. **34**, 173 (1951).
[26] L. G. Toth, H. Notwony, F. Benesovsky, and E. Rudy, Monatsh. Chem. **92**, 794 (1961).
[27] A. Zalkin and D. H. Templeton, Acta Cryst. **6**, 269 (1953).
[28] P. Blum and F. Bertaut, Acta Cryst. **7**, 81 (1954).

[29] H. C. Longuet-Higgins and M. de V. Roberts, Proc. Roy. Soc., **A224**, 336 (1954); **A230**, 110 (1955).
[30] D. W. Bullett, in *Boron-Rich Solids,* AIP Conf. Proc. 140, D. Emin, T. Aselage, C. L. Beckel, I. A. Howard, and C. Wood, Eds. (Am. Inst. Phys., New York, 1986), pp. 249–259.
[31] R. E. Rundle, N. C. Baenziger, A. S. Wilson, and R. A. McDonald, J. Am. Chem. Soc. **70**, 1718 (1948).
[32] For a review, see Z. Fisk, D. W. Hess, C. J. Pethick, D. Pines, J. L. Smith, J. D. Thompson, and J. O. Willis, Science **239**, 33 (1988).
[33] T. J. Heal and G. I. Williams, Acta Cryst. **8**, 494 (1955).
[34] R. C. Albers, A. M. Boring, and N. E. Christensen, Phys. Rev. **B33**, 8116 (1986).

Received May 6, 1991